Decentralized Control Model based Connected Automated Vehicle Trajectory Optimization of Mixed Traffic at An Isolated Signalized Intersection

Handong Yao, Xiaopeng Li*

Department of Civil and Environmental Engineering, University of South Florida, 4202 E Fowler Avenue, ENC 3300, Tampa, FL 33620

It is concerned that system-level benefits of connected automated vehicle control might only prevail in a far-future centralized control environment, whereas the benefits could be much offset in a near-future decentralized control system. To address this concern, this paper proposes a decentralized control model for connected automated vehicle trajectory optimization at an isolated signalized intersection with a single-lane road where each connected automated vehicle aims to minimize its own travel time, fuel consumption and safety risks. To improve the computational tractability, the original complex decentralized control model is reformulated into a discrete model. A benchmark centralized control model is also formulated to compare with the decentralized control model. The DIRECT algorithm is adopted to solve the above models. The numerical results show that the decentralized control model has better computational efficiency than the centralized control model without significant loss of the system optimality. Finally, analysis on connected automated vehicle market penetration shows that the extra benefit of the centralized control model is not obvious either in under-saturated traffic or at a low connected automated vehicle market penetration rate in critically-saturated and over-saturated traffic. The results suggest that, as apposed to the earlier concern, the near-future decentralized control scheme that requires less technology maturity and infrastructure investment can achieve benefits similar to the far-future centralized control scheme with much simple operations in under-saturated traffic, or in critically-saturated traffic and over-saturated traffic with a low connected automated vehicle market penetration rate.

Keywords: Decentralized control, Connected automated vehicle, Trajectory optimization, Signalized intersections, Mixed traffic.

1. Introduction

Connected Automated Vehicle (CAV) technologies are considered as promising technologies that can substantially improve traffic mobility, energy efficiency and safety. CAV

Email address: xiaopengli@usf.edu (Xiaopeng Li)

^{*}Corresponding author

enables timely communications between CAVs and infrastructures and precisely control of CAV trajectories. Especially, at bottlenecks (e.g., signalized intersections), CAV trajectory optimization can help vehicles pass signalized intersections without drastic acceleration and full stops to save travel time and energy. To date, a number of researchers have shown great interests in CAV trajectory optimization at intersections.

Early studies on CAV trajectory optimization at signalized intersections mainly focused on control of an individual vehicle alone (Asadi and Vahidi, 2011; Ahn et al., 2013; He et al., 2015; Xinkai Wu et al., 2015; Huang and Peng, 2017). Asadi and Vahidi (2011) designed a predictive cruise control with traffic signal information to improve fuel economy and trip time. Ahn et al. (2013) proposed an Eco-driving application to decrease fuel consumption. He et al. (2015) studied optimal vehicle speed trajectory considering both vehicle queue and traffic signal timing. Wu et al. (2015) extended energy-optimal trajectory control to electric vehicles. Huang et al. (2017) utilized sequential convex optimization to get the optimal vehicle trajectory. While these studies can help an individual vehicle save travel time and energy, the impacts of surrounding vehicles are not well addressed for the system-level optimality.

Since then, multiple-vehicle trajectory optimization methods including centralized control models (CM) and decentralized control models (DM) have been proposed to improve overall system performance. In CM, the decisions are made in a global manner for all vehicles by a single central controller. In DM, each vehicle is treated as an autonomous agent that determines its own control policy based on the information sensed or received from the other vehicles and road side units to maximize its own performance (Rios-torres and Malikopoulos, 2017).

Several research efforts addressed CM-based CAV trajectory optimization for maximizing system-level benefits at signalized intersections (Zhou et al., 2017; Ma et al., 2017; Wei et al., 2017; Zhao et al., 2018; Feng et al., 2018; He and Wu, 2018; Wang et al., 2018). Wei et al. (2017) proposed a dynamic programming-based vehicle trajectory optimization at a signalized intersection considering travel time as objective. Li et al. (2017, a; 2017, b) proposed a parsimonious shooting heuristic method for CAV trajectory control to optimize a multi-objective of travel time, fuel consumption and safety. Zhao et al. (2018) presented a cooperative Eco-driving model for mixed traffic. Feng et al. (2018) provided a joint optimization of vehicle trajectory control and signal control. Wang et al. (2018) came up with a cluster-wise eco-approach and departure (EAD) model at signalized corridors for minimizing fuel consumption. The above studies all used CM to smooth vehicles trajectories and improve traffic mobility, fuel efficiency or safety. Although CM can achieve the optimal system performance, it requires that all CAVs are compliant with the central controller, which often demands massive costs and future technologies for computation, communication and coordination.

Compared with CM, DM does not require such stringent operational settings and has a higher level of technology readiness for near-future traffic management. Makarem et al. (2013) mentioned that DM can significantly decrease computational and communication costs. A number of DM-based approaches have been proposed to address trajectory optimization problems at intersections (Makarem and Gillet, 2012; Makarem et al., 2013;

Campos et al., 2014; Zhang et al., 2016; Malikopoulos et al., 2018; Zhang and Cassandras, 2018; Mahbub et al., 2019; Zhang and Cassandras, 2019; Mirheli et al., 2019; Homchaudhuri et al., 2017; Jiang et al., 2017; Yang et al., 2017; Almutairi, 2016). Makarem and Gillet (2012) proposed a decentralized method for vehicles with smooth paths to avoid collisions. Further, Makarem and Gillet (2013) integrated model predicted control with decentralized control. Campos et al. (2014) formulated a local problem for each vehicle to avoid conflict at an unsignalized intersection. Zhang et al. (2016) optimized CAV trajectories along a signalfree corridor with an objective function incorporating vehicle accelerations. Almutairi and Rakha (2016) applied Eco-cooperative adaptive cruise control (CACC) system at signalized corridors. Yang et al. (2017) also came up with a method of Eco-CACC at signalized intersections considering queuing effect. Jiang et al. (2017) applied EAD method for mixed CAVs and manned vehicles traffic with simplified fuel consumption model. Homchaudhuri (2017) proposed a fast model predictive control-based fuel optimal trajectory planning method at signalized corridors. Malikopoulos et al. (2018) proposed a decentralized energy-optimal control at signal-free intersections with analytical solution methods. Zhang et al. (2018) added dynamic re-sequencing into decentralized control models to maximize traffic throughput and minimize energy at signal-free intersections. Zhang and Cassandras (2019) extended their previous work by considering all possible turns to optimize a passenger comfort metric with travel time and energy consumption. Mirheli et al. (2019) proposed a decentralized trajectory control model in unsignalized intersections for minimizing travel time, and compared it with a centralized model. Mahbub et al. (2019) conducted field experiments to implement the decentralized framework for CAVs with the optimal travel time and energy efficiency. While these DM studies demonstrated that decentralized control can reduce computation time, the performance of DM has not been quantitatively compared with that of CM and thus it is yet a pending question how much system optimality DM can achieve.

Further, most existing studies focus on pure CAV traffic, whereas near-future highway traffic is more likely mixed traffic with both CAVs and human driving vehicles (HVs) (which have completely different driving behaviors from CAVs). A number of studies have investigated the impact of mixed traffic in either DM or CM (Jiang et al., 2017; Yang et al., 2017; Zhao et al., 2018; Ghiasi et al., 2019; He and Wu, 2018; Homchaudhuri et al., 2017; Almutairi, 2016; Bergenhem et al., 2019). They verified that both DM and CM can yield benefits of CAV control in near-future mixed traffic. But the difference between DM and CM is not clarified in mixed traffic. Also, while CAV trajectory control pertains to mobility, energy and safety aspects of traffic systems, few studies investigate all three aspects holistically, particularly in the mixed traffic context.

Motivated by these research gaps, this paper proposes a DM-based CAV trajectory optimization for mixed traffic considering travel time, fuel consumption and safety at a signalized intersection. This model considers a single-lane segment with traffic approaching to an isolated signalized intersection. For each individual vehicle, we need to optimize its departure time and acceleration at each time step in the original decentralized model (OD). In order to simplify the OD, time discretization is applied to convert OD to a discrete decentralized model (DD) for finding the exact near-optimal solution. A benchmark CM is also formulated to compare with DM. CM is again reformulated into the discrete centralized model (DC)

in a similar manner. The DIRECT algorithm is adopted to solve the above models. The numerical results show that the extra improvement of CM is not significant in the system performance, and the computation time of DM is much less than CM. After that, mixed traffic including CAVs and HVs is considered. In the mixed traffic model, HVs are driven by a classic car-following model that is used to describe human driving behaviors, and CAVs are controlled by the corresponding CAV trajectory optimization algorithms. Finally, sensitivity analysis on CAV market penetration shows that the extra benefit of CM is not obvious in under-saturated traffic. In critically-saturated and over-saturated traffic, the extra benefit of CM is minor at a low CAV market penetration rate and is relatively high at intermediate and high CAV market penetration rates. The results suggest that DM requiring less technology maturity and infrastructure investment can achieve benefits similar to CM with much simple operations at all CAV market penetration rates in under-saturated traffic, or at a low CAV market penetration rate in critically-saturated traffic and over-saturated traffic.

Compared with the previous DM-based work, our study investigates a problem with several major differences. Instead of using a simple objective function (Zhang et al., 2017; Zhang and Cassandras, 2018, 2019; Homchaudhuri et al., 2017; Jiang et al., 2017) to reflect fuel consumption, a more detailed microscopic fuel consumption model (e.g., the VT-micro model (Ahn, 1998)) is applied in our study. And a joint objective of travel time, fuel consumption and safety is implemented to improve traffic mobility, energy efficiency and safety simultaneously. Different from the previous work that compares DM with a benchmark of traffic light control models (Zhang and Cassandras, 2019; Mirheli et al., 2019; Yang et al., 2017; Jiang et al., 2017), car following models (Zhang and Cassandras, 2018; Homchaudhuri et al., 2017) or single vehicle optimization models (Homchaudhuri et al., 2017; Jiang et al., 2017; Yang et al., 2017), a benchmark CM is formulated to show the comparison between DM and CM. While the previous work only considers a pure-CAV environment (Zhang and Cassandras, 2019; Zhang et al., 2017, 2016; Mirheli et al., 2019), mixed traffic of HVs and CAVs is studied with market penetration analysis in our study. To summarize, the contributions of this paper include the following aspects.

- 1) This paper proposes a DM-based CAV trajectory optimization model at an isolated signalized intersection with the aim of finding the optimal trajectories to minimize travel time, fuel consumption and safety risks simultaneously.
- 2) This paper compares DM with CM and verifies that DM yields better computational efficiency without much compromising solution optimality.
- 3) The effect of mixed traffic of CAVs and HVs is considered in this paper. The CAV market penetration analysis shows that the extra benefit of CM is not obvious in undersaturated traffic, or in critically-saturated and over-saturated traffic with a low CAV market penetration rate.

The organization of this paper is as follows. Section 2 formulates the original DM-based trajectory optimization model. A discretization method is used to reformulate the original DM and CM into discrete models in Section 3. Mixed traffic containing both CAVs and HVs is also investigated in Section 3. Section 4 conducts numerical experiments to investigate the applications of DM and CM at different traffic system settings and impacts of CAV market penetration on mixed traffic performance. Finally, Section 5 concludes this manuscript and

briefly discusses future research directions.

2. Problem Statement

This section proposes a DM-based CAV trajectory optimization model at a signalized intersection. For the convenience of readers, the key notation is summarized in Table 1.

Table 1: Notation list.

Notation	Definition
$\mathcal{N} \coloneqq [1, 2, \dots, N]$	Set of vehicles, where the number of vehicles is N .
$\mathcal{N}^C \coloneqq [1, 2, \dots, N^C]$	Set of CAVs, where the number of CAVs is N^C .
\mathcal{N}^{\prime}	Set of leading vehicles.
$\mathcal{K} \coloneqq [1, 2, \dots, K]$	Set of signal cycles in the planning horizon.
t	Index of time $t \in [0, T]$, where T is the maximum time.
i	Index of the time point at $i \times \theta$, where θ is the discrete-time interval.
$\mathcal{I} := [0, 1, 2,, I]$	Set of discrete-time points, where $I = \lceil T/\theta \rceil$.
n	Index of a vehicle, $n \in \mathcal{N}$.
k	Index of a signal cycle, $k \in \mathcal{K}$.
l_n^{veh}	Length of vehicle $n \in \mathcal{N}$.
h^C	Saturated time headway of CAV.
h^H	Saturated time headway of HV.
s^C	Minimum spacing of CAV.
s^H	Minimum spacing of HV.
$ au^C$	Time gap of CAV.
$ au^H$	Time gap of HV.
L	Location of stop-line, i.e., road segment length.
$\mathcal{X} := \left\{ X_n \right\}_{n \in \mathcal{N}}$	Set of vehicles trajectories.
$X_n = \left\{ x_n \left(t \right) \right\}_{t \in \mathcal{T}}$	Trajectory of vehicle $n \in \mathcal{N}$.
$x_{n}\left(t ight)$	Location of vehicle $n \in \mathcal{N}$ at time $t \in [0, T]$.
x_{ni}	Location of vehicle $n \in \mathcal{N}$ at discrete-time $i \in \mathcal{I}$.
_	Scheduled time point of vehicle $n \in \mathcal{N}$ at location 0, i.e., scheduled arriva
t_n^-	time.
\widetilde{t}_n^-	Actual time point of vehicle $n \in \mathcal{N}$ at location 0, i.e., actual arrival time.
$i\overline{n}$	Discretized arrival time of vehicle $n \in \mathcal{N}$, where $i_n^- = \lceil t_n^-/\theta \rceil$.
t_n^+	Time point of vehicle $n \in \mathcal{N}$ at location L , i.e., departure time.
i_n^+	Discretized departure time of vehicle $n \in \mathcal{N}$, where $i_n^+ = \begin{bmatrix} t_n^+/\theta \end{bmatrix}$.
$\dot{x}_{n}\left(t ight)$	Speed of vehicle $n \in \mathcal{N}$ at time $t \in [0, T]$.
v_{ni}	Speed of vehicle $n \in \mathcal{N}$ at discrete-time $i \in \mathcal{I}$.
v_n^+	Speed of vehicle $n \in \mathcal{N}$ at location L , i.e., departure speed.
\overline{v}	Maximum speed.
$\ddot{x}_n\left(t\right)$	Acceleration of vehicle $n \in \mathcal{N}$ at time $t \in [0, T]$.
	• • •

\overline{a}	Maximum acceleration.
\underline{a}	Minimum acceleration (or maximum deceleration with a negative sign).
G_k	Green length in signal cycle $k \in \mathcal{K}$.
R_k	Effective red length in signal cycle $k \in \mathcal{K}$.
C_k	Cycle length in signal cycle $k \in \mathcal{K}$, and $C_k = G_k + R_k$.
TT_n	Travel time of vehicle $n \in \mathcal{N}$.
D_n^-	Arrival delay of vehicle $n \in \mathcal{N}$.
FC_n	Fuel consumption of vehicle $n \in \mathcal{N}$.
SS_n	Safety surrogate measure of vehicle $n \in \mathcal{N}$.
J_n	Joint objective of vehicle $n \in \mathcal{N}$.
λ_T	Weight of travel time.
λ_D	Weight of arrival delay.
λ_F	Weight of fuel consumption.
λ_S	Weight of safety.

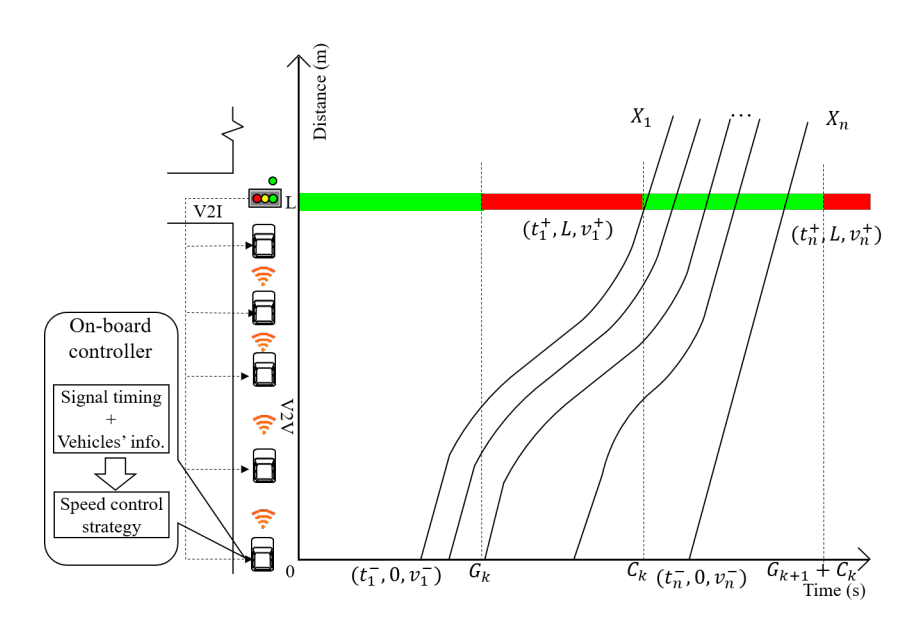


Figure 1: An Illustration of the decentralized control system.

See Figure 1, consider a platoon of vehicles indexed by $n=1,\ldots,N$ running on a single lane road segment with length L approaching a signalized intersection at the downstream end of the segment. Set location 0 as the entrance of the road segment and location L at the stop-line before the signalized intersection. For notation convenience, let $\mathcal{N}:=\{1,2,\ldots,N\}$ denote the set of vehicles. Consider time horizon $\mathcal{T}:=[0,T]$ for the trajectory optimization decisions. Let $t:=x_n^{-1}(l)$ denote the first time for vehicle n at location $l\in(-\infty,+\infty)$. Then $t_n^-:=x_n^{-1}(0)$ denotes the scheduled arrival time for vehicle $n\in\mathcal{N}$ at location 0, which we assume can be precisely predicted with upstream information. And $t_n^+:=x_n^{-1}(L)$ denotes the departure time of vehicle n at location L, which will depend on the decision variables.

We assume that the signal timing plan is pre-determined, and let $\mathcal{K} := \{1, 2, \dots, K\}$ denote the set of signal cycles within time horizon \mathcal{T} . In each signal cycle $k \in \mathcal{K}$, let G_k and R_k denote the effective green and red phase lengths, respectively, and let $C_k = G_k + R_k$ denote the corresponding cycle length. Without loss of generality, assume the signal begins a green phase at time 0, and thus the start time of cycle k is $(k-1) \times C_k$. Let $\mathcal{X} := \{X_n\}_{n \in \mathcal{N}}$ denote the set of time-space vehicle trajectories, where $X_n = \{x_n(t)\}_{t \in \mathcal{T}}$ is the trajectory of vehicle n and $x_n(t)$ denotes the location of vehicle n at time t. Let $\dot{x}_n(t) \in [0, \overline{v}]$ denote the speed of vehicle n at time t, where \overline{v} is the maximum speed. We assume that the arrival speed $v_n^- := \dot{x}_n(t_n^-)$ of vehicle n at location 0 can also be precisely predicted with upstream information. Let $v_n^+ := \dot{x}_n(t_n^+)$ denote the departure speed of vehicle n at location n, which will depend on the decision variables. And let $\ddot{x}_n(t) \in [\underline{a}, \overline{a}]$ denote the acceleration of vehicle n at time n, where n and n are the minimum and maximum acceleration rates of vehicle n, respectively.

Normally, vehicles without control will stop before the stop-line due to the interruption of red signal. In the decentralized control system, see Figure 1, vehicles can communicate with the surrounding environment (including signal lights and other CAVs) with Vehicle-to-Vehicle (V2V) and Vehicle-to-Infrastructures (V2I) technologies. And all CAVs are equipped with on-board controller that can control CAVs at each time and each location based on signal timing and vehicle information. In order to smooth vehicle trajectories for improving mobility, fuel efficiency and safety, CAVs will be controlled to have smoother trajectories without abrupt acceleration and deceleration before approaching a signalized intersection.

In DM, each individual vehicle controls its own trajectory to optimize its performance in terms of travel time, fuel consumption and safety risks with local information (e.g., from the preceding vehicle and infrastructure) subject to car following constraints. With this, DM with pure CAVs (i.e., all vehicles being CAVs) is formulated as follows.

For each vehicle $n \in \mathcal{N}$, the optimization objective is comprised of travel time, fuel consumption and safety components.

• Travel time: The travel time of vehicle n is formulated as

$$TT_n(X_n) = (t_n^+ - t_n^-) + \lambda_D D_n^-, \ \forall n \in \mathcal{N},$$
(1)

where λ_D is the weight of arrival delay. $D_n^- = \tilde{t}_n^- - t_n^-$ is the arrival delay of vehicle n, where \tilde{t}_n^- is the actual arrival time of vehicle n. At a light traffic, \tilde{t}_n^- is typically identical to the scheduled arrival time t_n^- . However, if "spillback" traffic occurs, i.e., when downstream slowdown shock wave spills back and forces upstream vehicles delay their arrivals, we may have $\tilde{t}_n^- > t_n^-$.

• Fuel consumption: The fuel consumption of vehicle n is the integral of the instantaneous fuel consumption function of speed and acceleration between the actual arrival time \tilde{t}_n^- and departure time t_n^+ . The formulation with the VT-micro fuel consumption model is as follows.

$$FC_n(X_n) = \int_{\tilde{t}_n^-}^{t_n^+} \exp\{\sum_{j_1=0}^3 \sum_{j_2=0}^3 K_{j_1 j_2} \dot{x}_n^{j_1}(t) \, \ddot{x}_n^{j_2}(t)\} dt, \, \forall n \in \mathcal{N},$$
 (2)

where j_1 and j_2 are the power indexes and, $K_{j_1j_2}$ is a constant coefficient. See Table 2 for the value of the coefficients (Zegeye et al., 2013).

Table 2: Coefficients for fuel consumption (the unit of fuel consumption, speed and acceleration are in $^{1}/_{s}$, $^{m}/_{s}$, and $^{m}/_{s}^{2}$, respectively).

$K_{j_1j_2}$	$j_2 = 0$	$j_2 = 1$	$j_2 = 2$	$j_2 = 3$
$j_1 = 0$	-7.537	0.4438	0.1716	-0.0420
$j_1 = 1$	0.0973	0.0518	0.0029	-0.0071
$j_1 = 2$	-0.0030	-7.42E-4	1.09E-4	1.16E-4
$j_1 = 3$	5.3E-5	6E-6	-1E-5	-6E-6

• Safety: The safety of vehicle n is measured by inverse time-to-collision based on Ma et al. (2017), as formulated below:

$$SS_n(X_n) = \int_{\tilde{t}_n^-}^{t_n^+} \max\left\{0, \frac{\dot{x}_n(t) - \dot{x}_{n-1}(t)}{x_{n-1}(t) - x_n(t) - l_{n-1}^{veh}}\right\} dt, \ \forall n \in \mathcal{N},\tag{3}$$

where l_{n-1}^{veh} is the length of vehicle $n \in \mathcal{N} \setminus \{1\}$. Since this paper assumes the traffic is homogeneous, we set $l_n^{veh} = l^{veh}$, $\forall n \in \mathcal{N}$. In order to make Equation (3) compatible with the first vehicle, set a dummy vehicle with $x_0(t) = \infty$ and $\dot{x}_0(t) = \overline{v}$, $\forall t \in \mathcal{T}$.

In addition, vehicle n should satisfy the following constraints.

• Departure time constraints: Departure time t_n^+ is bounded by a time range of $\left[\underline{t_n^+}, \overline{t_n^+}\right]$, i.e.,

$$\underline{t}_n^+ \le \underline{t}_n^+ \le \overline{t}_n^+, \ n \in \mathcal{N}. \tag{4}$$

Lower bound \underline{t}_n^+ is defined as follows,

$$\underline{t_n^+} = \mathcal{G}(\max\{t_n^- + \frac{(\overline{v} - \dot{x}_n(t_n^-))^2}{2\overline{a}\overline{v}} + \frac{L}{\overline{v}}, t_{n-1}^+ + \tau^C + \frac{s^C + l^{veh}}{\overline{v}}\}), \ \forall n \in \mathcal{N},$$
 (5)

where

$$\mathcal{G}(t) := \begin{cases} t, & \text{if} \mod(t, C) \in [0, G), \\ \lceil t/C \rceil \times C, & \text{otherwise.} \end{cases}$$
 (6)

 au^C and s^C are the minimum time gap and spacing between two consecutive CAVs, respectively. In order to make it available for the first vehicle, we assume $t_0^+ = -Inf$. If vehicle n accelerates to the maximum speed with the maximum acceleration and then cruises with the maximum speed to pass the intersection, we obtain $\underline{t_{n1}^+} = t_n^- + (\overline{v} - \dot{x}_n(t_n^-))^2/2\overline{av} + L/\overline{v}$. If vehicle n follows the preceding vehicle to pass the intersection, we obtain $\underline{t_{n2}^+} = t_{n-1}^+ + \tau^C + (s^C + l^{veh})/\overline{v}$. Then check the maximum value of $\underline{t_{n1}^+}$ and $\underline{t_{n2}^+}$. If this value falls in an effective green phase, set it as the lower bound departure time of $\underline{t_n^+}$. Otherwise, it hits a red light and will be pushed off to the beginning of the next effective green phase.

We assume that the departure time must be in an effective green time with a reasonable throughput. Hereinafter, upper bound departure time $\overline{t_n^+}$ is set as

$$\overline{t_n^+} = \min\left(\left\lfloor \frac{\underline{t_n^+}}{\overline{C}} \right\rfloor \times C + G, \underline{t_n^+} + \tau^C + \frac{s^C + l^{veh}}{\overline{v}} \right), \ \forall n \in \mathcal{N}.$$
 (7)

• Entry boundary constraints: Vehicle n arrives at location 0 at time \tilde{t}_n^- . Assume $\tilde{t}_0^- = 0$ to make the following equation compatible for the first vehicle,

$$\widetilde{t}_n^- \ge t_n^-, \ \forall n \in \mathcal{N}.$$
 (8)

$$x_n\left(\widetilde{t}_n^-\right) = 0, \ \forall n \in \mathcal{N}.$$
 (9)

• Exit boundary constraints: Vehicle n departs from location L at time t_n^+ ,

$$x_n\left(t_n^+\right) = L, \ \forall n \in \mathcal{N}.$$
 (10)

• Safety constraints: The minimum safety spacing is always ensured between two consecutive vehicles,

$$x_n(t) \le x_{n-1}(t - \tau^C) - (s^C + l^{veh}), \ \forall n \in \mathcal{N}, t \in \mathcal{T} \setminus \{0, \theta, 2\theta, \dots, \tau^C\},$$
 (11)

Since we assume $x_0(t) = Inf$, Equation (11) is applicable for the first vehicle.

• Speed constraints: Overtaking or backing up is not allowed,

$$0 \le \dot{x}_n(t) \le \overline{v}, \ \forall n \in \mathcal{N}, t \in \mathcal{T}. \tag{12}$$

• Acceleration constraints: Acceleration values are bounded in $[\underline{a}, \overline{a}]$,

$$\underline{a} \le \ddot{x}_n(t) \le \overline{a}, \ \forall n \in \mathcal{N}, t \in \mathcal{T}.$$
 (13)

Now, the original DM is formulated as N sub-problems of individual vehicles,

OD:
$$\min_{X_n} J_n^{\text{OD}}(X_n) := \lambda_T \times TT_n(X_n) + \lambda_F \times FC_n(X_n) + \lambda_S \times SS_n(X_n), \forall n \in \mathcal{N}, (14)$$

subject to Equations (4)-(13). In Equation (14), λ_T , λ_F and λ_S are the weights of travel time, fuel consumption and safety, respectively. Note that these sub-problems are linked with constraints (11). In actual driving, the decisions of down-stream vehicles are rarely affected by upstream ones, and thus, these sub-problems will be solved sequentially from the first vehicle upstream to the last vehicle. See Figure 2, it shows the optimization framework of the decentralized control system. Strictly speaking, sub-problem J_n^{OD} is solved after all downstream sub-problems J_1^{OD} , \cdots , J_{n-1}^{OD} are solved.

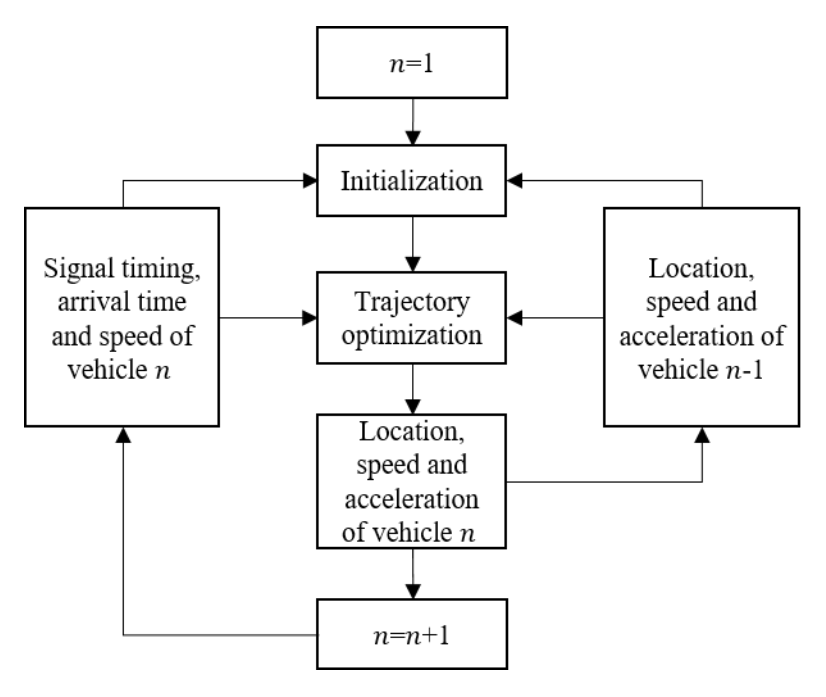


Figure 2: Optimization framework of the decentralized control system.

3. Discretization and Mixed Traffic Model

3.1 Discrete model

The OD model is difficult to be solved as the continuous time points where decision variables dwell lead to infinite dimensionality and the complex fuel consumption and safety objective terms impose high non-linearity. Thus, this section will reformulate OD as a discrete model (DD) to find an exact near-optimal solution.

Let $\mathcal{I} := [0, 1, 2, \dots, I]$ denote the set of discrete-time points with a discrete-time interval θ and a maximum discrete-time $I = T/\theta$. Let $i \in \mathcal{I}$ denote the index of a discrete-time point. Let $i_n^- := \left\lceil t_n^-/\theta \right\rceil$ and $\widetilde{i}_n^- := \left\lceil t_n^-/\theta \right\rceil$ denote the discretized scheduled and actual arrival time of vehicle $n \in \mathcal{N}$, respectively. Let $i_n^+ := \left\lceil t_n^+/\theta \right\rceil$ denote the discretized departure time of vehicle n. Let x_{ni} , v_{ni} and a_{ni} denote the location, speed and acceleration of vehicle n at discrete-time point i, respectively. Let $\mathcal{X}^I := \left\{ X_n^I \right\}$ denote the set of discretized time-space trajectories, where $X_n^I = \left\{ x_{ni} \right\}$ is the discretized time-space trajectory of vehicle n.

trajectories, where $X_n^I = \{x_{ni}\}$ is the discretized time-space trajectory of vehicle n. Then, Equation (1) is reformulated as $TT_n^{DD}\left(X_n^I\right) = t_n^+ - t_n^- + \lambda_D D_n^-$. Equation (2) is reformulated as $FC_n^{DD}\left(X_n^I\right) = \sum_{i_n^-}^{i_n^+} \exp\{\sum_{j_1=0}^3 \sum_{j_2=0}^3 K_{j_1j_2} v_{ni}^{j_1} a_{ni}^{j_2} \theta\}$. And Equation (3) is reformulated as $SS_n^{DD}\left(X_n^I\right) = \sum_{i_n^-}^{i_n^+} \max\{0, \frac{\theta \times \left(v_{ni} - v_{n(i-1)}\right)}{\left(v_{n(i-1)} - v_{ni} - l^{veh}\right)}\}$, $\forall n \in \mathcal{N}$. Set $x_{0i} = \infty$ and $v_{0i} = \overline{v}$, $\forall i \in \mathcal{I}$, thus it is applicable to the first vehicle.

For vehicle $n \in \mathcal{N}$, DD is formulated as follows,

DD:
$$\min_{X_n^I} J_n^{\text{DD}} \left(X_n^I \right) := \lambda_T \times TT_n^{DD} \left(X_n^I \right) + \lambda_F \times FC_n^{DD} \left(X_n^I \right) + \lambda_S \times SS_n^{DD} \left(X_n^I \right), \quad (15)$$

subject to

• Speed constraints:

$$v_{ni} = \frac{x_{ni} - x_{n(i-1)}}{\theta} \in [0, \overline{v}], \ \forall n \in \mathcal{N}, i \in \mathcal{I} \setminus \{0\}.$$
 (16)

• Acceleration constraints:

$$a_{ni} = \frac{v_{n(i+1)} - v_{ni}}{\theta} = \frac{x_{n(i+1)} - 2x_{ni} + x_{n(i-1)}}{\theta^2} \in [\underline{a}, \overline{a}], \ \forall n \in \mathcal{N}, i \in \mathcal{I} \setminus \{0, I\}.$$
 (17)

• Entry boundary constraint: Equation (8) and

$$x_{n\widetilde{i}_{n}} = v_{n}^{-} \times \left(\theta \times \widetilde{i}_{n}^{-} - \widetilde{t}_{n}^{-}\right), \ \forall n \in \mathcal{N}.$$

$$(18)$$

• Exit boundary constraint: Equation (8) and

$$x_{ni_n^+} = L + v_{ni_n^+} \times \left(\theta \times i_n^+ - t_n^+\right), \ \forall n \in \mathcal{N}. \tag{19}$$

• Safety constraints:

$$x_{ni} \le x_{(n-1)i}^s, \ \forall n \in \mathcal{N}, i \in \mathcal{I},$$
 (20)

where $x_{(n-1)i}^s$ is the shadow trajectory of vehicle n-1. It is formulated as

$$x_{(n-1)i}^s = x_{(n-1)(i-\Gamma^C)} - \left(s^C + l^{veh}\right) + v_{(n-1)(i-\Gamma^C)} \times \left(\Gamma^C \times \theta - \tau^C\right), \forall n \in \mathcal{N} \setminus \{1\}, i \in \mathcal{I}, (21)$$

where $\Gamma^C = \lceil \tau^C/\theta \rceil$ is the discretized time gap of CAV. In order to let Equation (20) work for the first vehicle, we set $x_{0i} = \infty$, $v_{0i} = \overline{v}$ and $a_{0i} = 0$, $\forall i \in \mathcal{I}$.

• Departure time constraints: Equations (4) - (7) and

$$t_n^+ = i_n^+ \times \theta - \frac{x_{ni_n^+} - L}{v_{ni_n^+}}, \ \forall n \in \mathcal{N}.$$
 (22)

Again, these sub-problems will be solved sequentially from the first vehicle upstream to the last vehicle.

To compare with DM, we also formulate a discrete model of the centralized control (DC) with measurements of the average system travel time $TT^{DC}\left(\mathcal{X}^{I}\right) = \frac{1}{N}\sum_{n=1}^{N}\left(t_{n}^{+} - t_{n}^{-} + \lambda_{D}D_{n}^{-}\right)$, the average system fuel consumption $FC^{DC}\left(\mathcal{X}^{I}\right) = \frac{1}{N}\sum_{n=1}^{N}FC_{n}^{DD}\left(X_{n}^{I}\right)$ and the average system safety $SS^{DC}\left(\mathcal{X}^{I}\right) = \frac{1}{N}\sum_{n=1}^{N}SS_{n}^{DD}\left(X_{n}^{I}\right)$.

DC:
$$\min_{\mathcal{X}^I} J^{\text{DC}}\left(\mathcal{X}^I\right) := \lambda_T \times TT^{DC}\left(\mathcal{X}^I\right) + \lambda_F \times FC^{DC}\left(\mathcal{X}^I\right) + \lambda_S \times SS^{DC}\left(\mathcal{X}^I\right).$$
 (23)

subject to Equations (16) - (21), and departure time constraints including Equation (22) and

$$t_n^+ \le t_n^+ \le \mathcal{T}, \ \forall n \in \mathcal{N},$$
 (24)

where
$$\underline{t_n^+} = \mathcal{G}(\max\{t_n^- + \frac{(\overline{v} - \dot{x}_n(t_n^-))^2}{2\overline{a}\overline{v}} + \frac{L}{\overline{v}}, \underline{t_{n-1}^+} + \tau^C + \frac{s^C + l^{veh}}{\overline{v}}\}).$$

$$t_n^+ \ge t_{n-1}^+ + \tau^C + \frac{s^C + l^{veh}}{\overline{v}}, \forall n \in \mathcal{N} \setminus \{1\}. \tag{25}$$

While DD and DC are bounded nonlinear problems, we use the Dividing Rectangles (DIRECT) method (Jones et al., 1993) to numerically search for near-optimal solutions. Shortly speaking, the DIRECT method is a sampling method that initially transform the domain of the problem into the unit hyper-cube and then divide the unit hyper-cube into smaller hyper-cubes with the sampling information. The detailed description of the DIRECT method can refer to Jones et al. (1993) and Finkel (2003). The initial solutions needed in the DIRECT method can be easily found by the shooting heuristic algorithm (Zhou et al., 2017; Ma et al., 2017) with selected start points $(\tilde{t}_n^-, \bar{a}_n^f, \underline{a}_n^f, v_n^f, \bar{a}_n^b, \underline{a}_n^b, v_n^+, t_n^+)$ for each vehicle $n \in \mathcal{N}$, where \bar{a}_n^f is the acceleration of forward shooting, \underline{a}_n^f is the deceleration of backward shooting, a_n^b is the acceleration of backward shooting, and \underline{a}_n^b is the deceleration of backward shooting.

3.2 Mixed traffic model

In this subsection, we consider the impacts of mixed traffic including CAVs and HVs in the near future. Let N^C and $N - N^c$ denote the number of CAVs and HVs, respectively. Let \mathcal{N}^C denote the set of CAVs. Thus, the market penetration rate (MPR) of CAVs can be represented by N^C/N . Assume that all HVs proceed according to the classic Gipps' model (Treiber and Kesting, 2013).

$$v_{n(i+\Gamma^{H})} = F^{Gipps}\left(v_{ni}, v_{(n-1)i}, s_{ni}\right) := \min \left\{v_{ni} + \overline{a} \times \Gamma^{H}, \overline{v}, \underline{a} \times \Gamma^{H} + \sqrt{\underline{a}^{2} \times (\Gamma^{H})^{2} + v_{(n-1)i}^{2} - 2 \times \underline{a} \times (s_{ni} - (s^{H} + l^{veh}))}\right\},$$

$$\forall n \in \mathcal{N} \setminus \mathcal{N}^{C}, i \in \left[0, I - \Gamma^{H}\right], \quad (26)$$

where τ^H is the time gap of HV and $\Gamma^H = \lceil \tau^H/\theta \rceil$ is the discretized time gap of HV. s^H is the minimum spacing of HV. $s_{ni} = x_{(n-1)i} - x_{ni}$ is the spacing between vehicle n and n-1 at discrete-time point i. Assume $v_{0i} = \overline{v}$ and $x_{0i} = \infty$, $\forall i \in \mathcal{I}$, Equation 26 works for the first vehicle. For HVs, they need to stop at a red light. And the queuing effect should be considered. Thus, the operation rules of HVs can be formulated as follows,

$$v_{n(i+\Gamma^{H})} = \begin{cases} F^{Gipps}\left(v_{ni}, v_{(n-1)i}, s_{ni}\right), & \text{if } \mod(t, C) \in [0, G), \\ \min\left\{F^{Gipps}\left(v_{ni}, v_{(n-1)i}, s_{ni}\right), F^{Gipps}\left(v_{ni}, 0, L - x_{ni}\right)\right\}, & \text{otherwise.} \end{cases}$$

$$\forall n \in \mathcal{N} \setminus \mathcal{N}^{\mathcal{C}}, i \in \left[0, I - \Gamma^{H}\right]. \quad (27)$$

Then, we can calculate acceleration a_{ni} and location x_{ni} of vehicle $n \in \mathcal{N} \setminus \mathcal{N}^C$ at discrete-time point $i \in [0, I - \Gamma^H]$ according to Equations (16) and (17).

Considering mixed traffic, Equations (5) and (21) are reformulated as

$$x_{(n-1)i}^{s} = \begin{cases} x_{(n-1)(i-\Gamma^C)} - \left(s^C + l^{veh}\right) + v_{(n-1)(i-\Gamma^C)} \times \left(\Gamma^C \times \theta - \tau^C\right), & \text{if } n \in \mathcal{N}^C, \\ x_{(n-1)(i-\Gamma^H)} - \left(s^H + l^{veh}\right) + v_{(n-1)(i-\Gamma^H)} \times \left(\Gamma^H \times \theta - \tau^H\right), & \text{otherwise.} \end{cases}$$
(28)

$$\underline{t_n^+} = \begin{cases} \mathcal{G}(\max\{t_n^- + \frac{\left(\overline{v} - \dot{x}_n(t_n^-)\right)^2}{2\overline{av}} + \frac{L}{\overline{v}}, t_{n-1}^+ + \tau^C + \frac{s^C + l^{veh}}{\overline{v}} \}), & \text{if } n \in \mathcal{N}^C, \\ \mathcal{G}(\max\{t_n^- + \frac{\left(\overline{v} - \dot{x}_n(t_n^-)\right)^2}{2\overline{av}} + \frac{L}{\overline{v}}, t_{n-1}^{s+} \}), & \text{otherwise.} \end{cases} \tag{29}$$

In Equation (29), $t_{n-1}^{s+}:=i_{n-1}^{s+}\times\theta-(x_{n-1}^{s+}-L)/v_{n-1}^{s+}$ is the departure time of shadow trajectory of vehicle n-1, where $x_{n-1}^{s+}:=\min_{i\in\mathcal{I},s.t.x_{(n-1)i}^s\geq L+\eta}\left(x_{(n-1)i}^s\right)$ is the near-location when the shadow trajectory of vehicle n-1 passes location L. $i_{n-1}^{s+}:= \mathrm{argmin}_{i\in\mathcal{I},s.t.x_{(n-1)i}^s\geq L+\eta}\left(x_{(n-1)i}^s\right)$ is the discrete-time point at location $x_{n-1}^{s+}.$ v_{n-1}^{s+} is the departure speed of the shadow trajectory of vehicle n-1. And η is an extremely small value (i.e., $1e^{-6}$ in this paper).

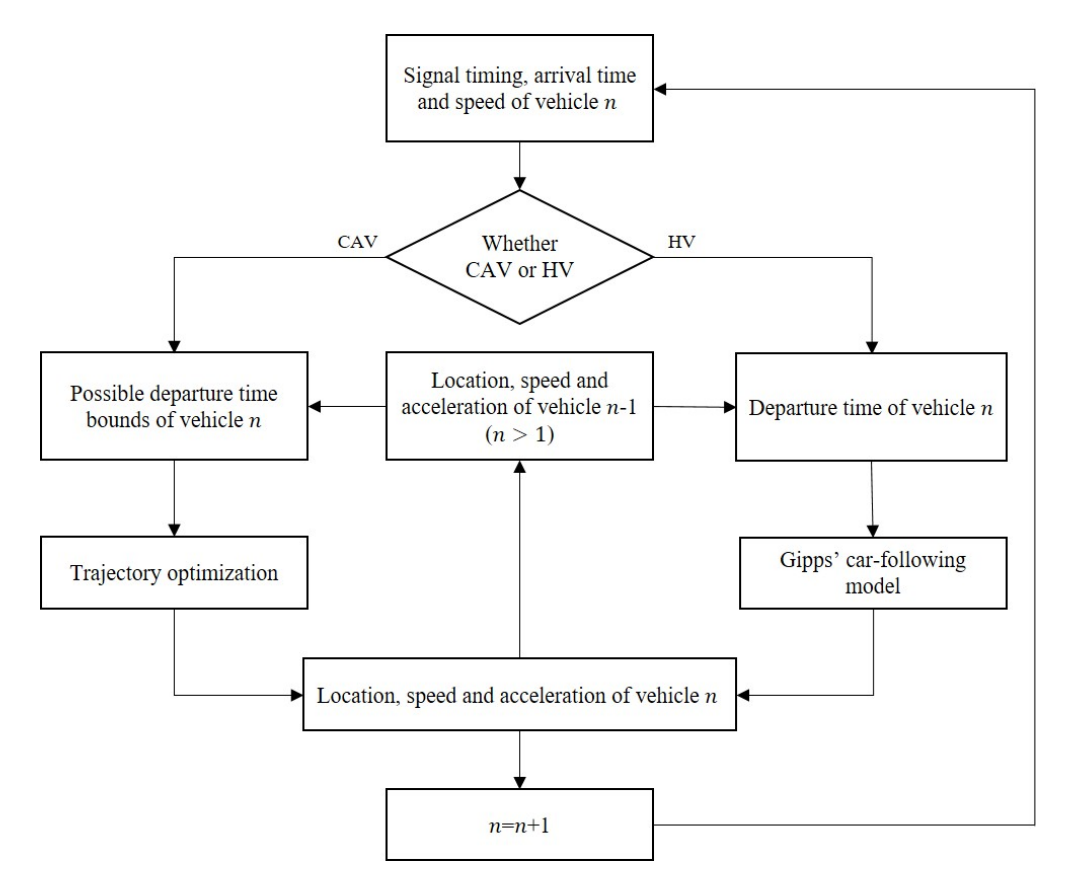


Figure 3: Control logic of the DM-based mixed traffic model.

Figure 3 plots the control logic of the proposed DM-based mixed traffic model. First, we need to identify whether vehicle n is a CAV or HV. If vehicle $n \in \mathcal{N}^C$, the corresponding trajectory optimization model is applied to obtain the location, speed and acceleration of vehicle n. If vehicle $n \in \mathcal{N} \setminus \mathcal{N}^C$, it would follow Gipps' car-following rules to calculate the location, speed and acceleration of vehicle n.

4. Numerical Experiments

This section tests the above proposed DM, CM and the mixed traffic model in a set of numerical experiments. The parameter settings are described in Subsection 4.1. The results of DM and CM are compared to investigate the effectiveness of DM under pure CAVs traffic in Subsection 4.2. The sensitivity analysis of CAV market penetration is conducted in Subsection 4.3 to investigate the impacts of mixed traffic.

4.1. Parameter settings

Parameters are set as following default values: The maximum time is $T=500\,\mathrm{s}$. The vehicle length is $l^{veh}=4\,\mathrm{m}$. The maximum speed is $\overline{v}=16\,\mathrm{m/s}$. The maximum acceleration is $\overline{a}=2\,\mathrm{m/s^2}$ and the minimum acceleration is $\underline{a}=-2\,\mathrm{m/s^2}$. we set the minimum CAV spacing as $s^C=1\,\mathrm{m}$ and the minimum CAV time gap as $\tau^C=0.7\,\mathrm{s}$. Assume that $G_k=G$, $R_k=R$, and $C_k=C=2\times G$, $\forall k\in\mathcal{K}$ to represent fixed-time signals. The number of signal cycles is K=T/C. Note that most vehicles may not be influenced by red lights and there is less stop-and-go traffic when we fix t_1^- in the setting of a long green length. Thus, we set t_1^- with a random value from [1,G] and generate the scheduled arrival times as $t_n^-=t_{n-1}^-+(\tau^C+(s^C+l_{veh})/\bar{v})\times(1+\xi_n\times(C/f^sG-1))$, $\forall n\in\mathcal{N}\setminus\{1\}$, where ξ_n is an uniformly distributed random number over [0,2] and $f^s\in(0,C/G]$ is the traffic saturation rate. Note that the scheduled arrival times may be pushed back after trajectory optimization, otherwise the safety constraints will be violated. Then, we generate v_n^- with a random value uniformly distributed over $[\overline{v}/2,\overline{v}]$ from vehicle 1 to vehicle N. When v_n^- violates the safety constraint, we let $v_n^-=v_{n-1}^-$ and $t_n^-=t_{n-1}^-+\tau+(s+l_{veh})/v_{n-1}^-$.

Similar to Ma et al. (2017), set $\lambda_T = \$20/h$ (weight of travel time), $\lambda_F = \$1/\text{liter}$ (weight of fuel consumption), and $\lambda_S = 0.1$ (weight of safety). And we try to find a robust $\lambda_D \in [1, 100]$ for both of the system arrival delay and system joint objective in DM under a set of problem scenarios with different parameter settings in under-saturated traffic ($f^s = 0.5$): the road segment lengths (L = 400, 800 and 1200 m) and the signal cycle lengths (C = 30, 60 and 90 s). The results are plotted in Figure 4. We notice that when $\lambda_D \geq 50$, both of the system arrival delay and system joint objective maintain at stable levels implying that any $\lambda_D \in [50, 100]$ can be a robust weight of arrival delay for the system joint objective and ensuring the system arrival delay is marginal in under-saturated traffic. Thus, we set $\lambda_D = 50$ in this study.

With all weights determined, we are ready to investigate the system performance of DM and CM. To generate feasible trajectories with a better solution quality for both DM and CM, the shooting heuristic algorithm starts at three selected points in parallel for each instance. These three start points have the same $\{\tilde{t}_n^-, \bar{a}_n^b, v_n^f, \underline{a}_n^f, \overline{a}_n^b, v_n^b, \underline{a}_n^b, v_n^b\} = \{t_n^-, \overline{a}, \underline{a}, \overline{v}, \overline{a}, \underline{a}, \overline{v}\}$

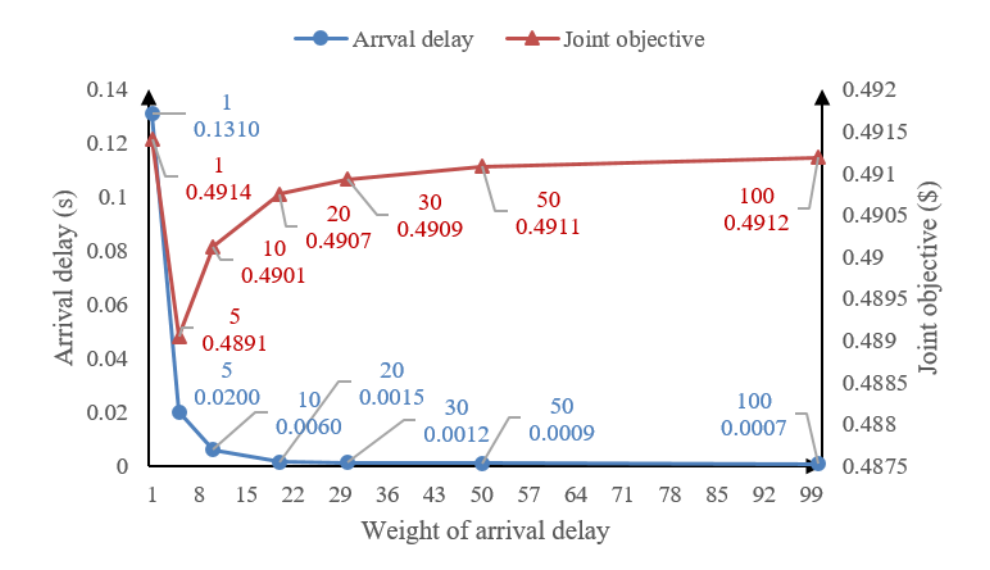


Figure 4: Determination of λ_D .

with three different $t_n^+ = \left\{ \underline{t_n^+}, \overline{t_n^+}, (\underline{t_n^+}, +t_n^+)/2 \right\}$ values. Figure 5 plots an illustration of the DIRECT method in DM with $L = 400\,\mathrm{m},\ C = 30\,\mathrm{s}$ and $f^s = 0.5$. We find that the DIRECT method is started with three different start points and then converge to near-optimal solutions. The lowest near-optimal solution (i.e., the red-circle curve) will be chosen as the final solution in this illustration.

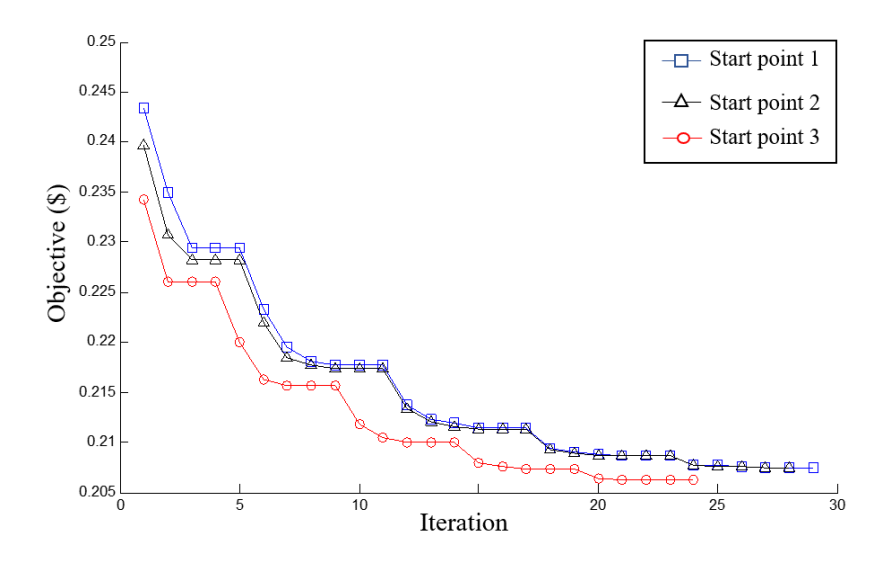


Figure 5: An illustration of the DIRECT method.

4.2. Comparison of DM and CM

In this subsection, the system performance results of DM and CM are investigated with sensitivity analysis experiments considering traffic levels, road segment lengths and signal cycle lengths. The traffic saturation rates range from 0.5 to 1.8 with an increment of 0.1. The road segment lengths range from 200 m to 1200 m with an increment of 200 m. And the signal cycle lengths range from 30 s to 120 s with an increment of 15 s. The other parameters are set as default.

Figure 6 plots three examples trajectories of DM and CM. Figures 6 (a) and (b) plot the trajectory results of DM and CM with $L=1200\,\mathrm{m},\,C=90\,\mathrm{s}$ and $f^s=0.5$, respectively. Figures 6 (c) and (d) plot the trajectory results of DM and CM with $L=800\,\mathrm{m},\,C=60\,\mathrm{s}$ and $f^s=1.0$, respectively. Figures 6 (e) and (f) plot the trajectory results of DM and CM with $L=400\,\mathrm{m},\,C=30\,\mathrm{s}$ and $f^s=1.5$, respectively. We see that the trajectory shapes of DM and CM are similar in the first example due to a low level of traffic saturation rate (i.e., under-saturated traffic). When the traffic saturation rate grows to an intermediate level (i.e., critically-saturated traffic), little "spillback" traffic occurs in both CM and DM, which is marked as blue-dotted line in Figure 6. Then, more "spillback" traffic occurs when the traffic saturation rate grows to a higher level (i.e., over-saturated traffic). Further, the trajectories in CM are more compact than those in DM under the critically-saturated traffic and over-saturated traffic. This indicates that CM can yield more benefits in the system travel time compared with DM.

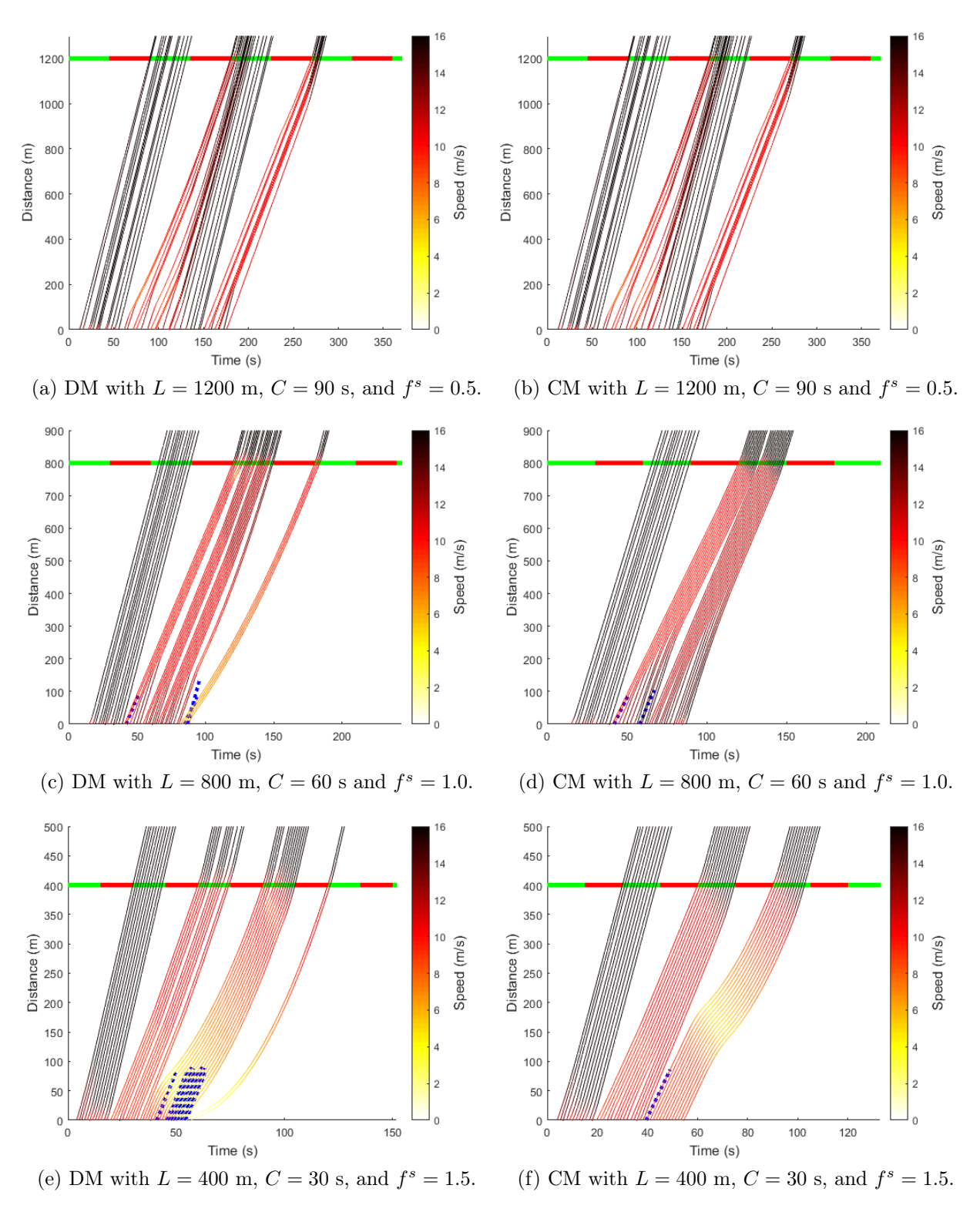


Figure 6: Examples of trajectory results of DM and CM.

Table 3: Comparison results of DM and CM. Notes: In each case, we run 5 times of DM and CM with stochastic arrival times and speeds to yield average results. J^{DM} and J^{CM} are the optimal system joint objective values for DM and CM, respectively; ΔJ^{CM-DM} is the extra improvement of CM v.s. DM; D^{DM-} and D^{CM-} are the system arrival delay caused by "spillback" traffic in DM and CM, respectively; T^{DM} is the solution time per vehicle in DM.

f^s	C (s)	<i>L</i> (m)	J^{DM} (\$)	J^{CM} (\$)	D^{DM-} (s)	D^{CM-} (s)	ΔJ^{CM-DM}	T^{DM} (s)
0.5	30	400	0.2703	0.2703	0.00	0.00	0.00%	13.70
		800	0.4529	0.4527	0.00	0.00	0.04%	14.02
		1200	0.6323	0.6308	0.00	0.00	0.24%	13.70
	60	400	0.3106	0.3106	0.00	0.00	0.00%	14.52
		800	0.4872	0.4870	0.00	0.0083	0.04%	14.37
		1200	0.6677	0.6672	0.00	0.00	0.07%	12.82
	90	400	0.4323	0.4321	0.0242	0.0037	0.05%	14.02
		800	0.5645	0.5628	0.0003	0.0031	0.30%	12.50
		1200	0.6425	0.6416	0.00	0.00	0.14%	12.72
Brie	f average				0.0027	0.0016	0.10%	13.60
1	30	400	0.3404	0.3072	0.0453	0.0056	9.75%	10.82
		800	0.5003	0.4759	0.0009	0.0003	4.88%	11.57
		1200	0.6785	0.6410	0.0005	0.0007	5.53%	14.47
	60	400	0.4021	0.3857	0.0133	0.0221	4.08%	15.52
		800	0.5208	0.5138	0.0001	0.0130	1.34%	10.1
		1200	0.7410	0.7258	0.0001	0.0081	2.05%	12.47
	90	400	0.4635	0.4446	0.0561	0.0158	4.08%	13.27
		800	0.5825	0.5665	0.0004	0.0225	2.75%	10.67
		1200	0.6985	0.6937	0.0002	0.00	0.69%	13.02
Brie	f average				0.0129	0.0097	3.90%	12.43
1.5	30	400	0.4722	0.3891	0.9465	0.1034	17.6%	4.77
		800	0.5485	0.4842	0.0913	0.0037	11.7%	4.95
		1200	0.6786	0.6403	0.0006	0.0009	5.64%	4.12
	60	400	0.4331	0.3735	0.2040	0.0114	13.7%	2.47
		800	0.4939	0.4698	0.0001	0.0352	4.88%	3.10
		1200	0.7876	0.7652	0.0116	0.0037	2.84%	5.72
	90	400	0.5634	0.5083	0.4080	0.1509	9.78%	5.20
		800	0.5008	0.4847	0.0153	0.0048	3.21%	4.95
		1200	0.6752	0.6741	0.0001	0.00	0.16%	3.55
Brie	f average				0.1864	0.0349	7.73%	4.32
Tota	al average				0.0673	0.0154	3.91%	10.11

Table 3 shows the comparison results of DM and CM with varying parameters. The total average extra improvement of CM is not significant (i.e., with an average of 3.91%). Especially, the extra improvement of CM can be ignored (i.e., with an average of 0.10%) in

the under-saturated traffic. With the traffic saturation rate grows, the extra improvement of CM becomes more obvious. The average values are 3.90% and 7.73% in the critically-saturated traffic and over-saturated traffic, respectively. We also find that the average arrival delay in both DM and CM become higher with the increasing traffic saturation rate. And the average arrival delay in CM is smaller than in DM, which indicates that CM has the ability to avoid serious "spillback" traffic. Furthermore, we find that DM is much better than CM in computation. The average solution time for each vehicle of DM and CM are about 10 s and 60 s, respectively. Note that, if a higher level computer with multiple cores and a simplified model with less decision variables are applied, the average solution time for each vehicle can be reduced to less than 1 s for DM. In conclusion, DM is much better than CM in computational efficiency without significant loss in the system optimality.

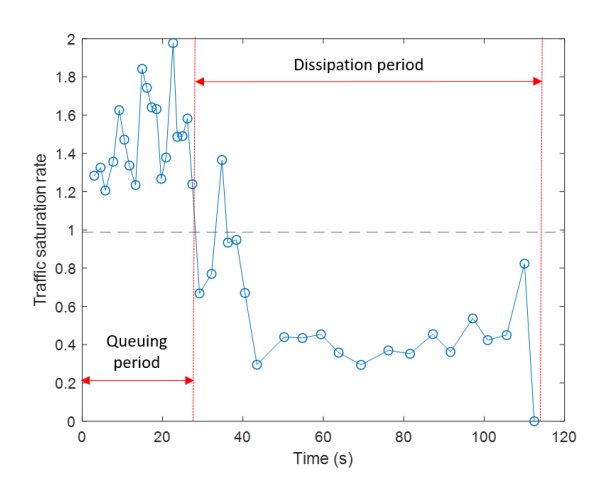


Figure 7: An illustration of the divided over-saturated traffic.

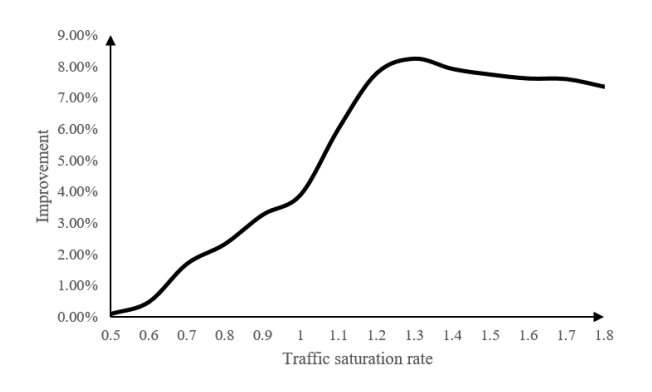
To better reflect the reality in the over-saturated traffic, we further divide the oversaturated period into two parts according to Sun et al. (2015): the queuing period when stop-and-go traffic occurs seriously at high traffic saturation rates; and the dissipation period when the stop-and-go traffic is dissipating gradually at low traffic saturation rates. Figure 7 plots an illustration of the divided over-saturated traffic. In this case, the first 20 vehicles arrive at high traffic saturation rates (with an average of 1.5), and the last 20 vehicles arrive at low traffic saturation rates (with an average of 0.5). And the black dashed line shows the average traffic saturation rate is around 1.0. Table 4 shows the comparison results between DM and CM in the divided over-saturated traffic. The average extra improvement of CM is 4.78%, which is smaller than in the over-saturated traffic (with an average of 7.73%) and a little bit higher than in the critically-saturated traffic (with an average of 3.90%). Because the stop-and-go traffic is dissipating in the dissipation period, the average arrival delay and the extra improvement of CM are smaller than those in the over-saturated traffic. Compared with the critically-saturated traffic, more stop-and-go movements occur in the queuing period, and thus the average arrival delay and the extra improvement of CM become higher. Further, the extra improvement of CM in the divided over-saturated traffic

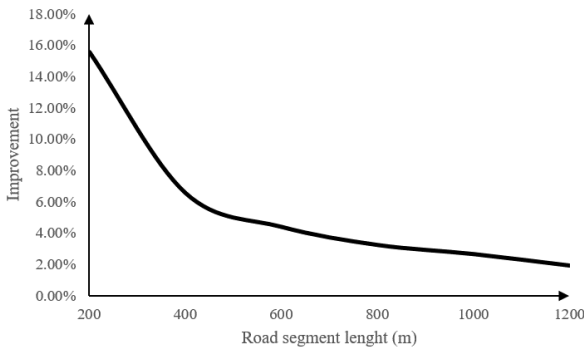
(the average traffic saturation rate is 1.0) is between the critically-saturated traffic (the traffic saturation rate is 1.0) and the over-saturated traffic (the traffic saturation rate is 1.5). With this understanding, the following analysis, with a focus on time-invariant traffic saturation rates, will investigate how different saturation rates impact the extra improvement of CM.

Table 4: Comparison result between DM and CM in the divided over-saturated traffic. Notes: the average traffic saturation rate is 1.0.

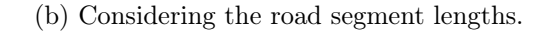
C (s)	<i>L</i> (m)	J^{DM} (\$)	J^{CM} (\$)	D^{DM-} (s)	D^{CM-} (s)	ΔJ^{CM-DM}
30	400	0.3409	0.2944	1.0605	0.0434	13.6%
	800	0.3930	0.3464	0.0613	0.0382	11.8%
	1200	0.4737	0.4382	0.0117	0.0001	7.49%
60	400	0.4829	0.4699	0.0013	0.0013	2.69%
	800	0.4979	0.4920	0.0002	0.0002	1.18%
	1200	0.5780	0.5756	0.0095	0.0040	0.42%
90	400	0.6743	0.6667	0.0014	0.0019	1.13%
	800	0.7635	0.7230	0.0005	0.0303	4.40%
	1200	0.6520	0.6517	0.0016	0.0100	0.05%
Average				0.1276	0.0144	4.76%

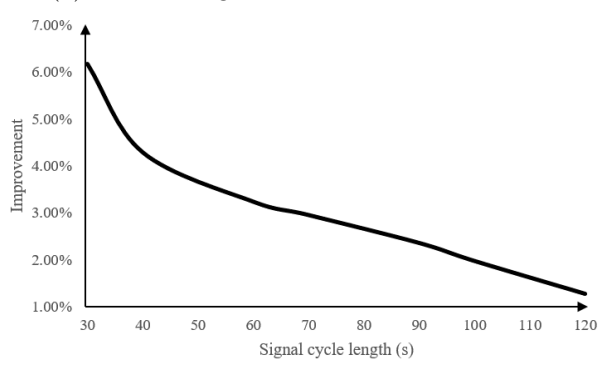
In order to understand the variation tendency of the extra improvement of CM, sensitivity analysis results with varying parameters are plotted in Figure 8. Figure 8 (a) indicates that the extra improvement of CM increases with a convex shape as the traffic saturation rate grows. That is to say the extra improvement of CM grows with the increasing traffic saturation rate until the traffic saturation rate reaches an intermediate level (i.e., $f_s \leq 1.3$); and then the extra improvement of CM drops a little with the further increasing traffic saturation rate (i.e., $f_s > 1.3$). Because DM only focuses on local optimization, the following vehicles may be affected by the local optimization of the subject vehicle and serious "spillback" traffic may form. However, CM focuses on global optimization considering all vehicles and thus can mitigate serious "spillback" traffic. When vehicles arrive with longer gaps at a lower traffic saturation rate, DM yields similar system optimality as CM with fewer negative effects on the following vehicles; and compared with DM at a higher traffic saturation rate, CM also has less room to regulate the trajectories and thus cannot yield further extra improvement. Figure 8 (b) plots that the extra improvement of CM decreases as the road segment length goes up. This is probably because vehicles have more room to be regulated with smoother trajectories (i.e., smaller speed variation) and thus DM causes less "spillback" traffic with smaller speed variations and yields similar system optimality as CM, when the road segment length becomes longer. Figure 8 (c) shows that the extra improvement of CM decreases as the signal cycle length increases. This is probably because a longer signal cycle length makes more vehicles pass a signalized intersection in one cycle and yields less stop-and-go traffic, and thus the extra improvement of CM becomes smaller. In reality, CM requires highly compliance of all CAVs and has stringent requirements on computation, communication and coordination. While DM slightly compromises system optimality, it is much easier to implement and circumvent the difficulty of enforcing individual vehicles to follow exact prescribed trajectories sent from a traffic management center. When the traffic saturation rate is low, the road segment length is long, and/or the signal cycle length is long, DM yields the similar system optimality as CM. Considering the cost and complexity in implementation, DM is suggested to be used in these conditions. However, if the system performance is the absolute priority and traffic is heavily congested, implementation of CM will yield further improvements of the system performance.





(a) Considering the traffic saturation rates.





(c) Considering the signal cycle lengths.

Figure 8: Sensitivity analysis with varying traffic saturation rates, road segment lengths and signal cycle lengths.

4.3. CAV market penetration analysis

In this subsection, CAV market penetration analysis is investigated to study the impacts of mixed traffic in DM and CM. The time gap of HV is set as $\tau^H = 1$ s, and the minimum spacing of HV is set as $s^H = 4$ m. Let $f^s = 0.5$, 1.0 and 1.5 to investigate the impacts of mixed traffic under different traffic saturation rates. The scheduled arrival times of HVs are set as $t_n^- = t_{n-1}^- + (\tau^H + (s^H + l_{veh})/\bar{v}) \times (1 + \xi_n \times (C/f^s G - 1))$, $\forall n \in \mathcal{N} \setminus \mathcal{N}^C$. The other parameters are set as default. Then, a set of CAV market penetration rates (i.e., $N^C/N = [0, 100\%]$) with an increment of 10%) is tested in the following experiments.

Table 5: CAV market penetration analysis results of DM and CM. Note: $\Delta J^{DM-MPR-0.5}$ and $\Delta J^{CM-MPR-0.5}$ are percent improvements in the cases of MPR> 0% v.s. benchmark (i.e., MPR= 0%) for DM and CM in the under-saturated traffic, respectively. $\Delta J^{DM-MPR-1.0}$ and $\Delta J^{CM-MPR-1.0}$ are percent improvements in the cases of MPR> 0% v.s. benchmark (i.e., MPR= 0%) for DM and CM in the critically-saturated traffic, respectively. $\Delta J^{DM-MPR-1.5}$ and $\Delta J^{CM-MPR-1.5}$ are percent improvements in the cases of MPR> 0% v.s. benchmark (i.e., MPR= 0%) for DM and CM in the over-saturated traffic, respectively. $\Delta J^{CM-DM-1.0}$ and $\Delta J^{CM-DM-1.5}$ are extra improvements of CM v.s. DM in the under-saturated traffic, critically-saturated traffic and over-saturated traffic, respectively.

MPR	0% (benchmark)	20%	40%	60%	80%	100%
$\Delta J^{DM-MPR-0.5}$	0.00%	7.84%	12.95%	17.39%	19.37%	23.75%
$\Delta J^{CM-MPR-0.5}$	0.00%	8.41%	13.45%	17.41%	19.40%	23.83%
$\Delta J^{CM-DM-0.5}$	0.00%	0.61%	0.58%	0.03%	0.04%	0.10%
$\Delta J^{DM-MPR-1.0}$	0.00%	14.28%	17.11%	20.76%	27.68%	29.55%
$\Delta J^{CM-MPR-1.0}$	0.00%	15.66%	19.31%	24.29%	30.72%	32.13%
$\Delta J^{CM-DM-1.0}$	0.00%	1.64%	2.66%	4.56%	4.36%	3.90%
$\Delta J^{DM-MPR-1.5}$	0.00%	21.62%	23.89%	25.26%	29.85%	35.81%
$\Delta J^{CM-MPR-1.5}$	0.00%	23.76%	27.25%	34.59%	37.08%	40.59%
$\Delta J^{CM-DM-1.5}$	0.00%	2.84%	4.46%	7.34%	8.29%	7.73%

Table 5 summaries CAV market penetration analysis results of DM and CM. 0% CAV MPR is the benchmark that all vehicles are HVs, and 100% CAV MPR is the pure CAVs traffic. All the improvements of DM and CM in different CAV MPRs compared to the benchmark can be found in Table 5 . For example, $J^{DM-MPR-0.5}$ and $J^{CM-MPR-0.5}$ are the improvements of DM and CM compared to the benchmark in the under-saturated traffic, respectively. First, we horizontally compare the results in Table 5. The improvements of DM and CM both increase as CAV MPR grows across all traffic saturation rates. This is because more controlled CAVs can further reduce the queuing effect of HVs as CAV MPR increases. Then, we vertically compare the results in Table 5. In the under-saturated traffic, the improvements are from 8% to 23%. In the critically-saturated traffic, the improvements are from 14% to 32%. And in the over-saturated traffic, the improvements are from 21% to 40%. This is because that more stop-and-go traffic occurs and both DM and CM yield better performance at a higher traffic saturation rate. Further, the extra improvements of CM are shown as $J^{CM-DM-0.5}$. $J^{CM-DM-1.0}$ and $J^{CM-DM-1.5}$ in the under-saturated traffic, critically-saturated traffic and over-saturated traffic, respectively. We find that the extra improvement of CM is marginal in the under-saturated traffic and becomes obvious in the critically-saturated traffic and over-saturated traffic.

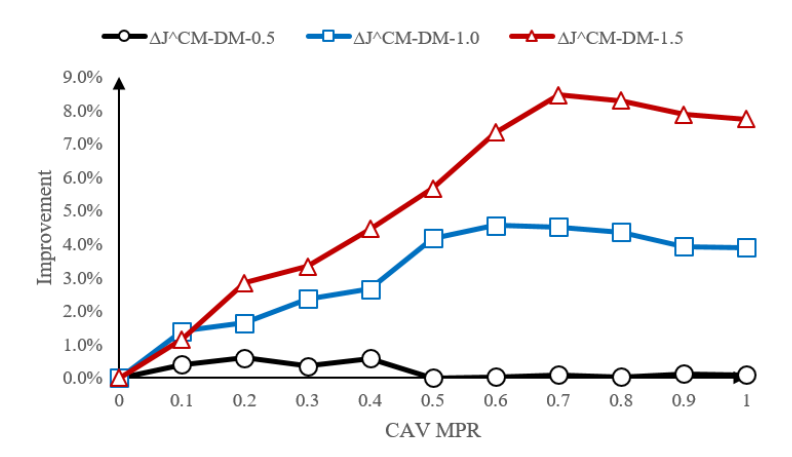


Figure 9: Extra improvements of CM v.s. DM with varying CAV MPRs.

Figure 9 plots the extra improvements of CM with varying CAV MPRs. The blackcircle curve, the blue-square curve and the red-triangle curve denote the extra improvements of CM in the under-saturated traffic, critically-saturated traffic and over-saturated traffic, respectively. First, we find that the extra improvement of CM is marginal (i.e., less than 1%) in the under-saturated traffic and becomes obvious in the critically-saturated traffic and over-saturated traffic. Additionally, an obvious variation tendency is found in the criticallysaturated and over-saturated traffic: the extra improvement of CM is marginal at a low CAV MPR; and then, it becomes significant at an intermediate CAV MPR; finally it drops a little at a high CAV MPR. That is because the impact of HVs is predominant at a low CAV MPR, and there is less potential for CM to improve. With CAV MPR increases, the impact of HVs decreases and both CM and DM yield significant benefit. However, DM only focuses on local optimization. CM focuses on the total system optimization, which considers more HV impacts and yields more benefits than DM with the increasing CAV MPR. When CAV MPR grows to a high level, DM can control more CAVs to decrease HV impacts and the extra improvement of CM drops a little. Therefore, the above results suggest that DM can be used in the under-saturated traffic instead of CM to improve computational efficiency without significant loss of the system optimality. In the critically-saturated traffic and over-saturated traffic, DM is welcomed to be used in a low level of CAV MPRs to decrease solution time, otherwise CM should be used to maintain the optimality of the system performance.

4.4. HV car following setting analysis

In this subsection, the effects of different HV car following settings with varying CAV MPRs are investigated. First, we investigate the effect of using the intelligent driver model (IDM) (Treiber and Kesting, 2013). The IDM is formulated as follows,

$$a_{ni} = F^{IDM}\left(v_{ni}, v_{(n-1)i}, s_{ni}\right) = \overline{a} \times \left(1 - \left(\frac{v_{ni}}{\overline{v}}\right)^{\delta} - \left(\frac{s_n^*\left(v_{ni}, v_{(n-1)i}\right)}{s_{ni}}\right)^2\right),$$

$$\forall n \in \mathcal{N} \setminus \mathcal{N}^C, i \in \left[0, I - \Gamma^H\right], \tag{30}$$

where $s_n^* \left(v_{ni}, v_{(n-1)i} \right) = s^H + \max \left\{ 0, v_{ni} \tau^H + v_{ni} \times \left(v_{ni} - v_{(n-1)i} \right) / 2 \sqrt{|\overline{a}\underline{a}|} \right\}$ is the desired gap, and δ is the exponent (set as 4 in general).

The IDM is tested in the critically-saturated traffic (i.e., $f^s=1$) with the same settings in subsection 4.3. Table 6 shows the results of the IDM and Gipps' model. We find that the improvements of using the IDM are higher than using Gipps' model. This is probably that vehicles will accelerate with the maximum acceleration due to the Equation (26) in the Gipps' model, but might accelerate with a value less than the maximum acceleration due to Equation (??) in the IDM. Thus, both DM and CM can yield more benefits by eliminating more "stop-and-go" traffic in the IDM than in the Gipps' model. Compared CM with DM, the extra improvement of using IDM shows a similar tendency as of using Gipps' model. We also find that $\Delta J^{CM-DM-IDM}$ is smaller than $\Delta J^{CM-DM-Gipps}$ at a low CAV MPR, and $\Delta J^{CM-DM-IDM}$ is larger than $\Delta J^{CM-DM-Gipps}$ at a high CAV MPR. Because the impact of HVs is predominant at a low CAV MPR and the IDM cause more "stop-and-go" traffic than the Gipps' model. Thus, the extra improvement of using the IDM is less than using the Gipps' model at a low CAV MPR. When the CAV MPR is high, CM can eliminate more "stop-and-go" traffic and thus $\Delta J^{CM-DM-IDM}$ is larger than $\Delta J^{CM-DM-Gipps}$.

Table 6: CAV market penetration analysis results of DM and CM with the IDM and Gipps' model in the critically-saturated traffic. Note: ΔJ^{DM-IDM} and ΔJ^{CM-IDM} are percent improvements in the cases of MPR> 0% v.s. benchmark (i.e., MPR= 0%) for DM and CM with the IDM, respectively. $\Delta J^{DM-Gipps}$ and $\Delta J^{CM-Gipps}$ are percent improvements in the cases of MPR> 0% v.s. benchmark (i.e., MPR= 0%) for DM and CM with the Gipps' model, respectively. $\Delta J^{CM-DM-IDM}$ and $\Delta J^{CM-DM-IDM}$ are extra improvements of CM v.s. DM with the IDM and the Gipps' model, respectively.

MPR	0% (benchmark)	20%	40%	60%	80%	100%
ΔJ^{DM-IDM} ΔJ^{CM-IDM}	0.00%	33.91%	40.52%	48.52%	52.72%	58.17%
ΔJ^{CM-IDM} $\Delta J^{CM-DM-IDM}$	0.00% 0.00%	34.90% 1.50%	43.79% 5.50%	52.33% 7.39%	55.91% 6.75%	60.79% 6.28%
$\Delta J^{DM-Gipps}$	0.00%	14.28%	17.11%	20.76%	27.68%	29.55%
$\Delta J^{CM-Gipps}$	0.00%	15.66%	19.31%	24.29%	30.72%	32.13%
$\Delta J^{CM-DM-Gipps}$	0.00%	1.64%	2.66%	4.56%	4.36%	3.90%

Then, we test the Gipps' model with different parameter settings (e.g., s^H) in the critically-saturated traffic under different CAV MPRs. The other settings are the same as in subsection 4.3. See Table 7, we find that the improvements of both CM and DM are decrease with the increasing s^H . This is probably that a lower s^H indicates a more aggressive driver and causes more "stop-and-go" traffic. Thus, DM and CM can yield more benefits by eliminating the "stop-and-go" traffic. Compared CM with DM, we find that the extra improvement of CM with different s^H shows a similar tendency. That is to say, s^H shows a marginal effect on the extra improvement between CM and DM. In conclusion, both DM and CM are capable to implement with different HV car following models and with different parameter settings.

Table 7: CAV market penetration analysis results of DM and CM with different s^H in the critically-saturated traffic. Note: ΔJ^{DM-6} and ΔJ^{CM-6} are percent improvements in the cases of MPR> 0% v.s. benchmark (i.e., MPR= 0%) for DM and CM with $s^H=6$ m, respectively. ΔJ^{DM-8} and ΔJ^{CM-8} are percent improvements in the cases of MPR> 0% v.s. benchmark (i.e., MPR= 0%) for DM and CM with $s^H=8$ m, respectively. ΔJ^{DM-15} and ΔJ^{CM-15} are percent improvements in the cases of MPR> 0% v.s. benchmark (i.e., MPR= 0%) for DM and CM with $s^H=15$ m, respectively. $\Delta J^{CM-DM-6}$, $\Delta J^{CM-DM-8}$ and $\Delta J^{CM-DM-15}$ are extra improvements of CM v.s. DM with $s^H=6$ m, $s^H=8$ m and $s^H=15$ m, respectively.

MPR	0% (benchmark)	20%	40%	60%	80%	100%
ΔJ^{DM-6}	0.00%	15.33%	21.80%	25.43%	30.76%	31.91%
ΔJ^{CM-6}	0.00%	17.54%	23.22%	27.61%	33.15%	34.92%
$\Delta J^{CM-DM-6}$	0.00%	1.94%	2.84%	4.54%	3.98%	3.87%
ΔJ^{DM-8}	0.00%	14.28%	17.11%	20.76%	27.68%	29.55%
ΔJ^{CM-8}	0.00%	15.66%	19.31%	24.29%	30.72%	32.13%
$\Delta J^{CM-DM-8}$	0.00%	1.64%	2.66%	4.56%	4.36%	3.90%
ΔJ^{DM-15}	0.00%	10.73%	14.73%	20.49%	23.00%	26.22%
ΔJ^{CM-15}	0.00%	11.23%	16.39%	24.26%	25.89%	29.09%
$\Delta J^{CM-DM-15}$	0.00%	1.66%	1.95%	4.73%	4.08%	3.89%

5. Conclusion

This paper proposes a DM-based CAV trajectory optimization model at an isolated signalized intersection with a single-lane road to smooth CAVs trajectories with a system joint objective including travel time, fuel consumption and safety. Then, discrete model is reformulated from the original DM to find the exact near-optimal solution. A benchmark CM is also formulated in a discrete model to compare with DM. The DIRECT method is applied to solve these two models with initial solutions generated from the shooting heuristic approach. Sensitivity analysis results show that DM is better than CM in computation efficiency without significant loss in the system optimality. The extra improvement of CM becomes more obvious as the traffic saturation rate increases, the road segment length decreases and the signal cycle length decreases. Further, the results of CAV market penetration analysis shows that the extra improvement of CM is marginal at a low CAV MPR; with CAV MPR increases, the extra improvement of CM increases; when CAV MPR approaches to 100% (i.e., the pure CAVs traffic), the extra improvement of CM drops a little. Therefore, either in the under-saturated traffic or at a low level of CAV MPRs in the critically-saturated traffic and over-critically traffic, DM is suggested to yield a faster computation efficiency with a similar system performance as CM; otherwise, CM is suggested to maintain the system optimality. Finally, we use a set of numerical experiments to verify that DM and CM are capable under different HV car following settings.

In the future, we will consider to extent the proposed decentralized control at a signalized intersection with a multi-lane road, where lane changing behaviors must be considered. Due to a larger gap generated by smoothed trajectories, vehicles in the adjacent lanes might change lane in front of CAVs, and thus might impair the system performance of trajectory optimization. Second, the trajectory optimization can be considered as a way to maximize the utility of space (e.g., smoothed trajectories). To maximize the utility of time, we will incorporate the trajectory optimization with a signal optimization. Additionally, we will extend the small scale problem (i.e., an isolated intersection) to a large scale problem (i.e., signalized corridor and urban network). A large scale problem may involve more complexities, e.g., origin and destination selection, route selection, and cooperation among multiple intersections, and might be hard to be solved. While we solve the large scale problem (e.g., multiple intersection cooperation), the spill back traffic in the decentralized control might be addressed. Further, the computation time of the proposed model is about 10 seconds that is still hard to implement in real-time control. Therefore, we will study other algorithms (e.g., piecewise approaximation) to improve the computation efficiency peer real-control needs.

Acknowledgment

This research is supported by the U.S. National Science Foundation through Grants CMMI #1558887 and CMMI #1932452.

References

- Ahn, K., 1998. Microscopic fuel consumption and emission modeling. Ph.D. thesis.
- Ahn, K., Rakha, H., Park, S., 2013. Ecodrive Application. Transportation Research Record: Journal of the Transportation Research Board 2341, 1–11. URL: http://trrjournalonline.trb.org/doi/10.3141/2341-01, doi:10.3141/2341-01.
- Almutairi, F., 2016. ECO-COOPERATIVE ADAPTIVE CRUISE CONTROL AT MULTIPLE SIGNALIZED INTERSECTIONS .
- Asadi, B., Vahidi, A., 2011. Predictive cruise control: Utilizing upcoming traffic signal information for improving fuel economy and reducing trip time. IEEE Transactions on Control Systems Technology 19, 707–714. doi:10.1109/TCST.2010.2047860.
- Bergenhem, C., Shladover, S., Coelingh, E., Englund, C., Tsugawa, S., Mirheli, A., Tajalli, M., Hajibabai, L., Hajbabaie, A., Aoki, S., Rajkumar, R.R., 2019. V2V-based Synchronous Intersection Protocols for Mixed Traffic of Human-Driven and Self-Driving Vehicles. 2019 IEEE 25th International Conference on Embedded and Real-Time Computing Systems and Applications (RTCSA) 100, 161–176. URL: https://doi.org/10.1016/j.trc.2019.01.004, doi:10.1109/RTCSA.2019.8864572.
- Campos, G.R., Falcone, P., Wymeersch, H., Hult, R., Sj, J., 2014. Cooperative receding horizon conflict resolution at traffic intersections. 53rd IEEE Conference on Decision and Control, 2932–2937doi:10.1109/CDC.2014.7039840.
- Feng, Y., Yu, C., Liu, H.X., 2018. Spatiotemporal intersection control in a connected and automated vehicle environment. Transportation Research Part C: Emerging Technologies 89, 364–383. URL: https://doi.org/10.1016/j.trc.2018.02.001https://linkinghub.elsevier.com/retrieve/pii/S0968090X1830144X, doi:10.1016/j.trc.2018.02.001.
- Finkel, D.E., 2003. DIRECT optimization user guide, 1–14.
- Ghiasi, A., Li, X., Ma, J., 2019. A mixed traffic speed harmonization model with connected autonomous vehicles. Transportation Research Part C 104, 210–233. URL: https://doi.org/10.1016/j.trc.2019.05.005, doi:10.1016/j.trc.2019.05.005.
- He, X., Liu, H.X., Liu, X., 2015. Optimal vehicle speed trajectory on a signalized arterial with consideration of queue. Transportation Research Part C: Emerging Technologies 61, 106–120. URL: http://dx.doi.org/10.1016/j.trc.2015.11.001, doi:10.1016/j.trc.2015.11.001.

- He, X., Wu, X., 2018. Eco-driving advisory strategies for a platoon of mixed gasoline and electric vehicles in a connected vehicle system. Transportation Research Part D 63, 907–922. URL: https://doi.org/10.1016/j.trd.2018.07.014, doi:10.1016/j.trd.2018.07.014.
- Homchaudhuri, B., Vahidi, A., Pisu, P., 2017. Fast Model Predictive Control-Based Fuel Efficient Control Strategy for a Group of Connected Vehicles in Urban Road Conditions 25, 760–767.
- Huang, X., Peng, H., 2017. Speed trajectory planning at signalized intersections using sequential convex optimization, in: 2017 American Control Conference (ACC), IEEE. pp. 2992–2997. URL: http://ieeexplore.ieee.org/document/7963406/, doi:10.23919/ACC.2017.7963406.
- Jiang, H., Hu, J., An, S., Wang, M., Park, B.B., 2017. Eco approaching at an isolated signalized intersection under partially connected and automated vehicles environment. Transportation Research Part C: Emerging Technologies 79, 290–307. URL: http://dx.doi.org/10.1016/j.trc.2017.04.001https://linkinghub.elsevier.com/retrieve/pii/S0968090X17301067, doi:10.1016/j.trc.2017.04.001.
- Jones, D.R., Law, C., Law, C., 1993. Lipschitzian Optimization Without the Lipschitz Constant 79.
- Ma, J., Li, X., Zhou, F., Hu, J., Park, B.B., 2017. Parsimonious shooting heuristic for trajectory design of connected automated traffic part II: Computational issues and optimization. Transportation Research Part B: Methodological 95, 421–441. URL: http://dx.doi.org/10.1016/j.trb.2016.06.010, doi:10.1016/j.trb.2016.06.010.
- Mahbub, A.M.I., Malikopoulos, A.A., Karri, V., Parikh, D., Jade, S., 2019. A Decentralized Time- and Energy-Optimal Control Framework for Connected Automated Vehicles: From Simulation to Field Test arXiv:arXiv:1911.01380v1.
- Makarem, L., Gillet, D., 2012. Fluent coordination of autonomous vehicles at intersections. 2012 IEEE International Conference on Systems, Man, and Cybernetics (SMC), 2557–2562doi:10.1109/ICSMC. 2012.6378130.
- Makarem, L., Gillet, D., Member, S., 2013. Model predictive coordination of autonomous vehicles crossing intersections. 16th International IEEE Conference on Intelligent Transportation Systems (ITSC 2013), 1799–1804doi:10.1109/ITSC.2013.6728489.
- Malikopoulos, A.A., Cassandras, C.G., Zhang, Y.J., 2018. A decentralized energy-optimal control framework for connected automated vehicles at signal-free intersections. Automatica 93, 244–256. URL: https://doi.org/10.1016/j.automatica.2018.03.056https://linkinghub.elsevier.com/retrieve/pii/S0005109818301511, doi:10.1016/j.automatica.2018.03.056, arXiv:1602.03786.
- Mirheli, A., Tajalli, M., Hajibabai, L., Hajbabaie, A., 2019. A consensus-based distributed trajectory control in a signal-free intersection. Transportation Research Part C 100, 161–176. URL: https://doi.org/10.1016/j.trc.2019.01.004, doi:10.1016/j.trc.2019.01.004.
- Rios-torres, J., Malikopoulos, A.A., 2017. A Survey on the Coordination of Connected and Automated Vehicles at Intersections and Merging at Highway On-Ramps. IEEE Transactions on Intelligent Transportation Systems 18, 1066–1077. doi:10.1109/TITS.2016.2600504.
- Sun, W., Wang, Y., Yu, G., Liu, H.X., 2015. Quasi-optimal feedback control for a system of oversaturated intersections. Transportation Research Part C 57, 224–240. URL: http://dx.doi.org/10.1016/j.trc.2015.06.018, doi:10.1016/j.trc.2015.06.018.
- Treiber, M., Kesting, A., 2013. Traffic Flow Dynamics. doi:10.1007/978-3-642-32460-4.
- Wang, Z., Member, S., Wu, G., Member, S., Hao, P., Barth, M.J., 2018. Cluster-Wise Cooperative Eco-Approach and Departure Application for Connected and Automated Vehicles Along Signalized Arterials 3 404–413
- Wei, Y., Avcı, C., Liu, J., Belezamo, B., Aydın, N., Li, P., Zhou, X., 2017. Dynamic programming-based multi-vehicle longitudinal trajectory optimization with simplified car following models. Transportation Research Part B: Methodological 106, 102–129. URL: https://doi.org/10.1016/j.trb.2017.10.012https://linkinghub.elsevier.com/retrieve/pii/S0191261517301078, doi:10.1016/j.trb.2017.10.012.
- Xinkai Wu, Xiaozheng He, Guizhen Yu, Harmandayan, A., Yunpeng Wang, 2015. Energy-Optimal Speed Control for Electric Vehicles on Signalized Arterials. IEEE Transactions on Intelligent Transportation Systems 16, 2786–2796. URL: http://ieeexplore.ieee.org/document/7097732/, doi:10.1109/TITS.2015.2422778.

- Yang, H., Rakha, H., Ala, M.V., 2017. Eco-Cooperative Adaptive Cruise Control at Signalized Intersections Considering Queue Effects. IEEE Transactions on Intelligent Transportation Systems 18, 1575–1585. URL: http://ieeexplore.ieee.org/document/7590076/, doi:10.1109/TITS.2016.2613740.
- Zegeye, S.K., Schutter, B.D., Hellendoorn, J., Breunesse, E.A., Hegyi, A., 2013. Integrated macroscopic traffic flow, emission, and fuel consumption model for control purposes. Transportation Research Part C 31, 158–171. URL: http://dx.doi.org/10.1016/j.trc.2013.01.002, doi:10.1016/j.trc.2013.01.002.
- Zhang, Y., Cassandras, C.G., 2018. A Decentralized Optimal Control Framework for Connected Automated Vehicles at Urban Intersections with Dynamic Resequencing. arXiv:1809.00262 [math] URL: http://arxiv.org/abs/1809.00262, arXiv:1809.00262.
- Zhang, Y., Cassandras, C.G., 2019. Automatica Decentralized optimal control of Connected Automated Vehicles at signal-free intersections including comfort-constrained turns and. Automatica 109, 108563. URL: https://doi.org/10.1016/j.automatica.2019.108563, doi:10.1016/j.automatica.2019.108563.
- Zhang, Y., Malikopoulos, A.A., Cassandras, C.G., 2017. Decentralized optimal control for connected automated vehicles at intersections including left and right turns, in: 2017 IEEE 56th Annual Conference on Decision and Control (CDC), IEEE. pp. 4428–4433. URL: http://ieeexplore.ieee.org/document/8264312/, doi:10.1109/CDC.2017.8264312, arXiv:1703.06956.
- Zhang, Y.J., Malikopoulos, A.A., Cassandras, C.G., 2016. Optimal control and coordination of connected and automated vehicles at urban traffic intersections. Proceedings of the American Control Conference 2016-July, 6227–6232. doi:10.1109/ACC.2016.7526648, arXiv:1509.08689.
- Zhao, W., Ngoduy, D., Shepherd, S., Liu, R., Papageorgiou, M., 2018. A platoon based cooperative ecodriving model for mixed automated and human-driven vehicles at a signalised intersection. Transportation Research Part C: Emerging Technologies 95, 802–821. URL: https://linkinghub.elsevier.com/retrieve/pii/S0968090X18307423, doi:10.1016/j.trc.2018.05.025.
- Zhou, F., Li, X., Ma, J., 2017. Parsimonious shooting heuristic for trajectory design of connected automated traffic part I: Theoretical analysis with generalized time geography. Transportation Research Part B: Methodological 95, 394–420. URL: http://dx.doi.org/10.1016/j.trb.2016.05.007, doi:10.1016/j.trb.2016.05.007, arXiv:1511.04810.